Journal of Solid State Chemistry **155,** 409–416 (2000)
doi:10.1006/jssc.2000.8942, available online at http://www.idealibrary.com on IDEAL®

Hydrothermal Synthesis and Crystal Structures of $[(CH_3NH_3)_{0.5}(NH_4)_{1.5}]Sb_8S_{13}\cdot 2.8H_2O$ and $Rb_2Sb_8S_{13}\cdot 3.3H_2O$

Xiqu Wang,[1] Lumei Liu, and Allan J. Jacobson

Department of Chemistry, University of Houston, Houston, Texas 77204-5641

Recived May 8, 2000; in revised form July 27, 2000; accepted August 17, 2000; published online November 29, 2000

The new thioantimonates $[CH_3NH_3)_{0.5}(NH_4)_{1.5}Sb_8S_{13}\cdot 2.8H_2O$ (1) and $Rb_2Sb_8S_{13}\cdot 3.3H_2O$ (2) have been hydrothermally synthesized and characterized by single-crystal structure determination. The two compounds are isostructural and crystallize in the monoclinic system, space group $P2_1/m$ with $a = 7.1931(3)$ Å, $b = 25.770(1)$ Å, $c = 15.9999(8)$ Å, $\beta = 96.856(1)^\circ$, $Z = 4$ for 1 and $a = 7.1899(8)$ Å, $b = 25.760(3)$ Å, $c = 15.973(2)$ Å, $\beta = 96.541(2)^\circ$, $Z = 4$ for 2, measured at 293 K. The structure consists of 12-membred rings of SbS_3 pyramids that are linked into one-dimensional complex chains. The chains are interconnected by secondary Sb–S bonds to form puckered layers. The stacking of the layers aligns the 12-membred rings, giving rise to a system of wide channels with an aperture of ca. 5.9 × 8.0 Å. The monovalent cations and water molecules are located in the channels. The layers are closely related to those found in the known compounds $(C_4H_{10}N)_2Sb_8S_{13}\cdot 0.15H_2O$ and $(C_8N_4H_{26})_{0.5}Sb_7S_{11}$. © 2000 Academic Press

Key Words: **antimony sulfide; thioantimonate; hydrothermal synthesis; crystal structure.**

INTRODUCTION

Open-framework chalcogenidometalates have attracted considerable interest because these porous frameworks also show semiconducting behavior and photoconductivity. (1–3). The synthesis and structural aspects of such compounds have been thoroughly reviewed recently (4, 5). Solvothermal methods are known to be very successful in synthesizing alkali metal thioantimonates (6–15). More recently, a large number of thioantimonates(III) with open-framework structures were synthesized under low-temperature hydrothermal conditions by using organic templates (16–27). Despite the structural complexity of many of the known phases, some systematic structural relationships have been recognized (5, 22). In a number of thioantimonates(III) the coordination environment of Sb can be considered as a hemioctahedron with different degrees of distortion. The hemioctahedra are often interconnected through edge-sharing into fragments that are similar to a two-atom-thick (100) slice in the NaCl structure. The fragments are further interconnected into slabs, layers, and frameworks. For a given framework (complex anion) composition, variations in the fragments and their linking often lead to very different structures. For example, the compounds $(enH_2)Sb_8S_{13}$ (18), $(C_4H_{10}N)_2Sb_8S_{13}\cdot 0.15H_2O$ (21), and $(CH_3NH_3)_2Sb_8S_{13}$ (19) have one-, two-, and three-dimensional structures, respectively. New examples of similar compounds will provide insight into their general structural chemistry.

Here we report two novel compounds $[(CH_3NH_3)_{0.5}(NH_4)_{1.5}]Sb_8S_{13}\cdot 2.8H_2O$ (**1**) $Rb_2Sb_8S_{13}\cdot 3.3H_2O$ (**2**) which are isostructural and which adopt a new structure type.

EXPERIMENTAL

Compounds **1** and **2** were hydrothermally synthesized by using elemental Sb and S. In a typical synthesis of **1**, Sb (0.37 g, 3 mmol) and S (1.00 g, 31 mmol) were mixed with 2.0 ml of a 40 wt% aqueous CH_3NH_2 solution. The mixture was sealed in a Teflon-lined autoclave (23 ml inner volume) in air and heated at 190°C for 4 days. Compound **2** was synthesized from a mixture of Sb (0.22 g, 1.8 mmol), S (0.10 g, 3.1 mmol), Rb_2CO_3 (0.63 g, 2.7 mmol), and H_2O (1.0 ml). The mixture was heated first at 90°C for 3 days and then at 190°C for 1 day. The products were washed with water, filtered, and dried in air.

Chemical compositions were analyzed with a JEOL 8600 electron microprobe operating at 15 KeV with a 10-μm beam diameter and a beam current of 30 nA. Infrared spectra were collected on a Galaxy FTIR 5000 spectrometer using the KBr pellet method. Thermogravimetric analyses were carried out in a nitrogen flow with a heating rate of 2°C/min, on a DuPont 2100 system.

Single-crystal X-ray data were measured on a SMART platform diffractometer equipped with a 1K CCD area detector using graphite-monochromatized Mo$K\alpha$ radiation

[1]To whom correspondence should be addressed. Fax: 713-7432787. E-mail: wangx@bayou.uh.edu.

0022-4596/00 $35.00

at room temperature. For each phase a hemisphere of data (1271 frames at 5 cm detector distance) was collected using a narrow-frame method with scan widths of 0.30° in ω and an exposure time of 30 s/frame. The first 50 frames were remeasured at the end of data collection to monitor instrument and crystal stability, and the maximum correction applied on the intensities was $<1\%$. The data were integrated using the Siemens SAINT program (28). Absorption correction was made using the program SADABS.(29). The structures were solved by direct methods and refined using SHELXTL (30). The discrimination between ammonium nitrogen and water oxygen atoms was made, not unambiguously, by considering interatomic distances and by comparing the two structures. The water oxygen atoms were constrained to have the same but a variable thermal parameter in order to refine their relative occupancies. Hydrogen atoms were ignored because of the large number of heavy atoms and partial occupancies of the water oxygen positions. Crystallographic and refinement details are summarized in Table 1. Atom positions are given in Tables 2 and 3.

RESULTS AND DISCUSSION

Synthesis and Characterization

Red needles of **1** with crystal sizes up to $1.5 \times 0.1 \times 0.1$ mm were obtained as a major phase together with minor impurities of $(CH_3NH_3)_2Sb_8S_{13}$. The yield is about 95% based on antimony. It was found that increasing the Sb:S mole ratio from about 1:10 to 2:3 substantially decreases the yield and the crystal sizes of **1**, and favors the formation of $(CH_3NH_3)_2Sb_8S_{13}$. Lowering the synthesis temperature has a similar effect. $(CH_3NH_3)_2Sb_8S_{13}$ is the major phase in a synthesis with an Sb:S ratio of 2:3 at a temperature of 130°C. The high temperature apparently increases the decomposition of methylamine and thus increases the ammonium concentration in the solution. Efforts to synthesize single-phase products by varying the Sb:S ratio and temperature were unsuccessful. Red needles of compound **2** could be obtained only as a minor phase in our syntheses. The yield is about 3% based on antimony. Other phases in the products include $RbSb_3S_5 \cdot H_2O$ (11) and amorphous powder.

The electron microprobe analysis gave the atomic ratios Sb:S = 8:12.7 for **1** and Sb:S:Rb = 8:12.8:1.9 for **2**, which are consistent with the formula ratios derived from structure refinements. The crystals of both compounds are not stable under an electron beam, which may account for the low measured S contents.

The observed IR bands for **1** at 1256(w), 1404(s), 1468(m), and 1616(s), and a very broad band between 2800 and 3700 cm^{-1}, indicate the existence of $CH_3NH_3^+$, NH_4^+, and water molecules. Figure 1 shows the TGA result for compound **1**. The gradual weight loss of 2.0% that ends at about 130°C is interpreted as partial dehydration and corresponds to $1.6H_2O$ per formula unit. The sharp weight loss between

TABLE 1
Crystal Data and Structure Refinement for $[(CH_3NH_3)_{0.5}(NH_4)_{1.5}]$ $Sb_8S_{13} \cdot 2.8H_2O$ (1) and $Rb_2Sb_8S_{13} \cdot 3.3H_2O$ (2)

	1	2
Formula	$H_{14.6}C_{0.5}N_2O_{2.8}S_{13}Sb_8$	$H_{6.6}O_{3.3}Rb_2S_{13}Sb_8$
F.W.	1484.3	1621.1
Temperature	293(2) K	293(2) K
Space group	$P2_1/m$	$P2_1/m$
Unit cell dimensions	$a = 7.1931(3)$ Å	$a = 7.1899(8)$ Å
	$b = 25.770(1)$ Å	b = 25.760(3) Å
	$c = 15.9999(8)$ Å	c = 15.973(2) Å
	$\beta = 96.856(1)°$	$\beta = 96.541(2)°$
Volume, Z	2944.6(2) $Å^3$, 4	2939.1(6) $Å^3$, 4
Density (calculated)	3.348 Mg/m^3	3.663 Mg/m^3
Wavelength	0.71073 Å	0.71073 Å
Absorption coefficient	8.153 mm^{-1}	11.458 mm^{-1}
Crystal size	$0.27 \times 0.04 \times 0.03$ mm	$0.52 \times 0.02 \times 0.01$ mm
$2\theta_{max}$	57°	57°
Reflections collected	17,610	18,495
Independent reflections	6796 [R(int) = 0.0421]	6956 [R(int) = 0.0918]
Data/restraints/parameters	6796/2/230	6955 / 0 / 228
Goodness-of-fit on F^2	1.082	0.978
R indices [$I > 2\sigma(I)$][a]	$R1 = 0.0441$, w$R2 = 0.0769$	$R1 = 0.0552$, w$R2 = 0.1137$
R indices (all data)[a]	$R1 = 0.0722$, w$R2 = 0.0869$	$R1 = 0.1031$, w$R2 = 0.1287$
Extinction coefficient	0.00019(2)	0.00007(4)
Largest diff. peak and hole	1.805 and -1.274 e $Å^{-3}$	2.096 and -1.599 e $Å^{-3}$

Note. [a] $R1 = \sum||F_o| - |F_c||/\sum|F_o|$. w$R2 = [\sum(w(F_o^2 - F_c^2)^2)/\sum(wF_o^2)^2]^{1/2}$. $w = 1/[\sigma^2(F_o^2) + (0.0211P)^2 + 23.7549P]$ for **1** and $w = 1/[\sigma^2(F_o^2) + (0.04997P)^2]$ for **2**, where $P = (F_o^2 + 2F_c^2)/3$

TABLE 2
Atomic Coordinates ($\times 10^4$) and Equivalent Isotropic Displacement Parameters ($Å^2 \times 10^3$) for $[(CH_3NH_3)_{0.5}(NH_4)_{1.5}]Sb_8S_{13} \cdot 2.8H_2O$ (1)

	x	*y*	*z*	*U*(eq)[a]	Occupancy
Sb(1)	8748(1)	3993(1)	1417(1)	20(1)	1
Sb(2)	3759(1)	4092(1)	2039(1)	22(1)	1
Sb(3)	2836(1)	4443(1)	− 1515(1)	22(1)	1
Sb(4)	4652(1)	3373(1)	104(1)	22(1)	1
Sb(5)	7950(1)	4623(1)	− 881(1)	23(1)	1
Sb(6)	2033(1)	5149(1)	− 3724(1)	24(1)	1
Sb(7)	9947(1)	3248(1)	− 998(1)	22(1)	1
Sb(8)	2842(1)	4645 (1)	4102(1)	22(1)	1
S(1)	3893(5)	2500	− 517(2)	25(1)	1
S(2)	7800(3)	3140(1)	726(1)	20(1)	1
S(3)	6165(3)	4461(1)	640(1)	19(1)	1
S(4)	7056(3)	3731(1)	− 1476(1)	21(1)	1
S(5)	2218(3)	3819(1)	3305(1)	25(1)	1
S(6)	4554(3)	4721(1)	− 2833(1)	23(1)	1
S(7)	9982(3)	4876(1)	− 2116(1)	21(1)	1
S(8)	6947(3)	3867(1)	2688(1)	21(1)	1
S(9)	814(3)	4314(1)	− 82(1)	19(1)	1
S(10)	3077(3)	3232(1)	1397(1)	24(1)	1
S(11)	1409(3)	4334(1)	− 4683(1)	26(1)	1
S(12)	3953(3)	5604(1)	− 4684(1)	22(1)	1
S(13)	1770(3)	3574(1)	− 2119(2)	25(1)	1
S(14)	8813(5)	2500	− 1917(2)	34(1)	1
N(1)	6881(20)	2500	2493(10)	59(4)	1
C(1)	8953(24)	2500	2742(18)	108(9)	1
N(2)	4198(21)	2500	− 2582(9)	56(4)	1
N(3)	1979(16)	6155(5)	− 6523(7)	68(3)	1
OW1	4501(20)	3373(6)	− 3771(9)	133(4)	1
OW2A	5559(58)	2950(15)	− 5862(27)	133(4)	0.41(2)
OW2B	4690(76)	3017(18)	− 5397(33)	133(4)	0.33(2)
OW2C	2726(86)	2898(21)	− 5193(36)	133(4)	0.26(2)
OW3	1148(35)	6796(10)	− 4922(16)	133(4)	0.59(2)
OW4	− 261(78)	7500	− 6125(35)	133(4)	0.37(3)

Note. [a] *U*(eq) is defined as one-third of the trace of the orthogonalized U_{ij} tensor.

TABLE 3
Atomic Coordinates ($\times 10^4$) and Equivalent Isotropic Displacement Parameters ($Å^2 \times 10^3$) for $Rb_2Sb_8S_{13} \cdot 3.3H_2O$ (2)

	x	*y*	*z*	*U*(eq)	Occupancy
Sb(1)	8741(1)	3995(1)	1418(1)	21(1)	1
Sb(2)	3742(1)	4106(1)	2035(1)	23(1)	1
1Sb(3)	2848(1)	4436(1)	− 1516(1)	22(1)	1
Sb(4)	4702(1)	3370(1)	108(1)	22(1)	1
Sb(5)	7960(1)	4616(1)	− 874(1)	23(1)	1
Sb(6)	2057(1)	5150(1)	− 3708(1)	24(1)	1
Sb(7)	9999(1)	3246(1)	− 982(1)	23(1)	1
Sb(8)	2817(1)	4653 (1)	4111(1)	23(1)	1
S(1)	3944(6)	2500	− 504(3)	25(1)	1
S(2)	7813(4)	3139(1)	759(2)	22(1)	1
S(3)	6180(4)	4458(1)	640(2)	23(1)	1
S(4)	7101(4)	3721(1)	− 1456(2)	23(1)	1
S(5)	2188(4)	3838(1)	3301(2)	28(1)	1
S(6)	4572(4)	4717(1)	− 2837(2)	25(1)	1
S(7)	1(4)	4867(1)	− 2119(2)	22(1)	1
S(8)	6904(4)	3877(1)	2685(2)	23(1)	1
S(9)	814(4)	4315(1)	− 82(2)	21(1)	1
S(10)	3055(4)	3246(1)	1398(2)	26(1)	1
S(11)	1393(4)	4340(2)	− 4672(2)	30(1)	1
S(12)	3987(4)	5599(1)	− 4679(2)	23(1)	1
S(13)	1820(4)	3570(1)	− 2107(2)	26(1)	1
S(14)	8879(7)	2500	− 1904(4)	37(1)	1
Rb(1)	6504(3)	2500	2547(2)	50(1)	1
Rb(2)	4221(3)	2500	7380(2)	49(1)	1
Rb(3)	2004(2)	6169(1)	− 6521(1)	57(1)	1
OW1	5701(20)	6671(7)	− 6088(11)	105(3)	1
OW2	625(29)	2500	2754(16)	105(3)	1
OW3	5229(20)	3036(7)	4353(11)	105(3)	1
OW4	1060(27)	6806(9)	− 4769(14)	105(3)	0.78(3)

Note. [a] *U*(eq) is defined as one-third of the trace of the orthogonalized U_{ij} tensor.

200–250°C indicates decomposition of the compound. A total weight loss of 9.1% below 250°C was observed, in reasonable agreement with the value calculated for loss of methylamine, ammonia, water, and H_2S (8.5%). Hydrolysis of sulfide by part of the water present in the structure during decomposition may account for the slightly higher observed weight loss. The presence of water in the structure after the initial dehydration stage is confirmed by the IR spectrum measured on a sample after thermogravimetric analysis that was ended at 135°C. X-ray powder diffraction analysis indicates that the framework of compound **1** is not substantially changed after partial dehydration below 135°C.

CRYSTAL STRUCTURES

The local coordination environments of Sb atoms of compound **1** are shown in Fig. 2. Selected bond lengths and bond angles for **1** are listed in Table 4. All eight nonequivalent Sb atoms are each coordinated by three nearest sulfur atoms to form trigonal pyramids with Sb–S

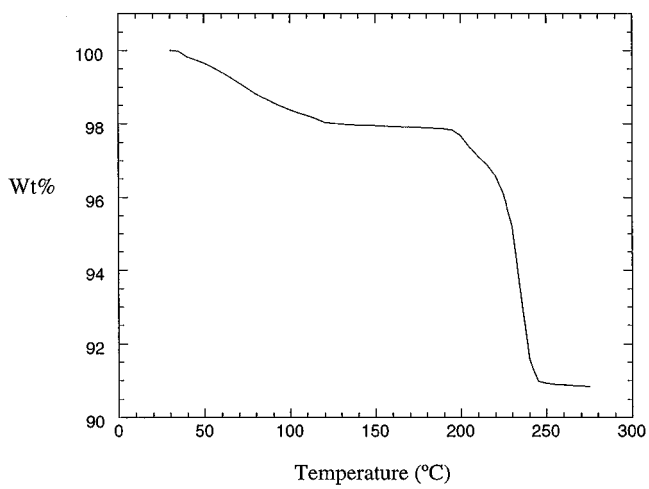

FIG. 1. TGA result for $[(CH_3NH_3)_{0.5}(NH_4)_{1.5}]Sb_8S_{13} \cdot 2.8H_2O$.

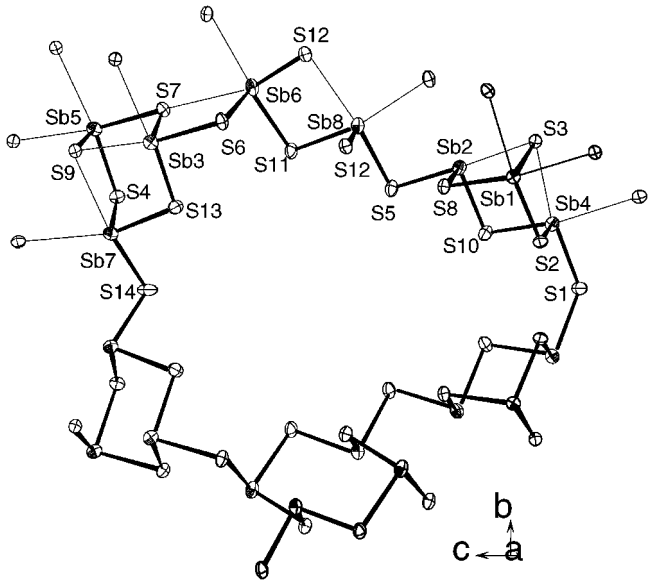

FIG. 2. A fragment of the structure of $[(CH_3NH_3)_{0.5}(NH_4)_{1.5}]Sb_8S_{13}\cdot 2.8H_2O$, showing the atom labeling scheme. Thermal ellipsoids are at 50% probability. Thick and thin solid lines represent Sb–S bond lengths in the ranges 2.42–2.68 and 2.88–3.36 Å, respectively.

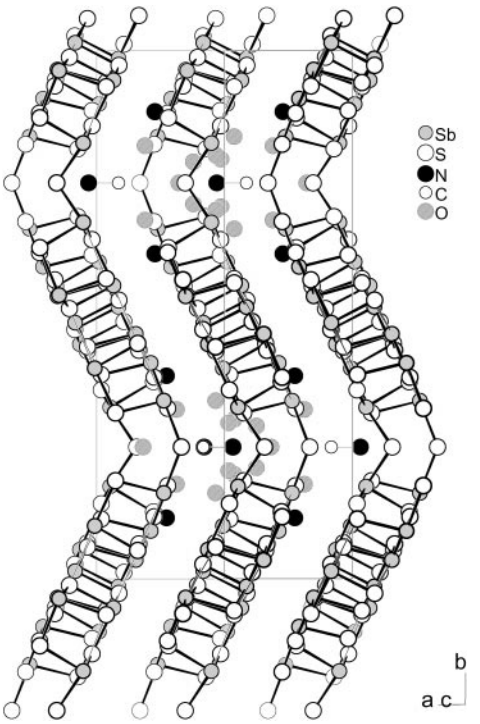

FIG. 4. Projection along [10-1] of the structure of $[(CH_3NH_3)_{0.5}(NH_4)_{1.5}]Sb_8S_{13}\cdot 2.8H_2O$.

bond lengths between 2.425 and 2.676 Å and S–Sb–S angles in the range of 87.9–98.4°. The coordination environments of Sb(1) and Sb(3–8) are each complemented by two additional S atoms, and that of Sb(2) by one, with Sb–S distances between 2.88 and 3.36 Å.

If only the short Sb–S bonds (2.42–2.68 Å) are considered, the $[SbS_3]$ trigonal pyramids are interconnected into complex infinite chains along [010] through sharing their

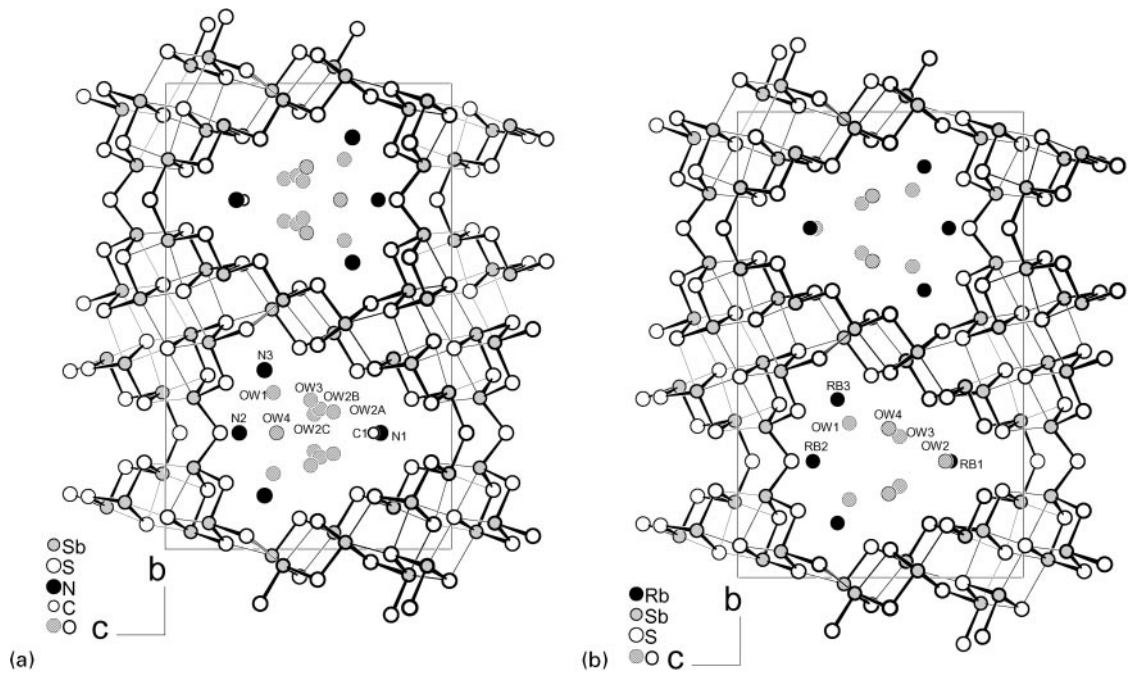

FIG. 3. Projection along [100] of the structures of (a) $[(CH_3\ NH_3)_{0.5}(NH_4)_{1.5}]Sb_8S_{13}\cdot 2.8H_2O$ and (b) $Rb_2Sb_8S_{13}\cdot 3.3H_2O$.

common S corners. The pyramids [Sb(1,2,4)S_3] and [Sb(3,5,7)S_3] form 3-membered rings, respectively. Such 3-membered rings are linked with the pyramids [Sb(6,8)S_3] to form large 12-membered rings that have a mirror plane symmetry (Figs. 2, 3). The 12-membered rings are interconnected into the [010] complex chain by the [Sb(6,8)S_3] pyramids that form 4-membered rings. Adjacent 12-membered rings are linked by an inversion symmetry center at

TABLE 4
Selected Bond Lengths (Å) and Angles (°) for $[CH_3NH_3)_{0.5}(NH_4)_{1.5}]]Sb_8S_{13} \cdot 2.8H_2O$ (1) (First Row) and $Rb_2Sb_8S_{13} \cdot 3.3H_2O$ (2) (Second Row)

	Distance	Angles			
Sb1–					
S3	2.429(2)				
	2.416(3)				
S2	2.518(2)	93.31(7)			
	2.502(3)	93.9(1)			
S8	2.558(2)	92.35(7)	95.86(7)		
	2.558(3)	91.9(1)	95.2(1)		
S9	3.083(2)	83.03(6)	91.29(7)	171.71(7)	
	3.075(3)	82.84(9)	92.2(1)	171.2(1)	
S7	3.214(2)	84.06(7)	174.28(7)	89.33(7)	83.36(6)
	3.230(4)	84.1(1)	175.3(1)	89.1(1)	83.42(9)
Other S	> 3.68				
	3.66				
Sb2–					
S10	2.467(2)				
	2.464(4)				
S8	2.470(2)	95.33(8)			
	2.461(3)	95.2(1)			
S5	2.521(2)	89.95(8)	94.16(8)		
	2.516(4)	89.9(1)	93.9(1)		
S3	3.137(2)	94.26(7)	78.88(6)	172.16(7)	
	3.122(3)	94.0(1)	78.71(9)	171.9(1)	
S6	3.475(3)	170.53(7)	77.69(7)	96.88(7)	78.22(5)
	3.458(4)	170.72(9)	77.7(1)	96.4(1)	78.94(8)
Other S	> 3.79				
	3.79				
Sb3–					
S7	2.432(2)				
	2.430(3)				
S13	2.521(2)	93.01(8)			
	2.501(4)	93.4(1)			
S6	2.666(2)	90.76(7)	94.83(8)		
	2.666(3)	90.5(1)	95.0(1)		
S9	2.877(2)	83.40(7)	92.44(7)	170.90(7)	
	2.871(3)	83.3(1)	92.8(1)	170.3(1)	
S3	3.197(2)	84.40(7)	174.13(7)	90.47(7)	82.05(6)
	3.215(3)	84.2(1)	174.1(1)	90.4(1)	81.63(9)
Other S					
	> 3.54				
	3.56				
Sb4–					
S2	2.437(2)				
	2.431(3)				
S1	2.493(2)	95.10(9)			
	2.482(2)	95.6(1)			
S10	2.502(2)	96.70(8)	95.7(1)		
	2.511(3)	96.6(1)	96.1(1)		
S3	3.091(2)	80.26(7)	169.08(9)	94.67(7)	
	3.082(3)	80.4(1)	169.6(1)	94.0(1)	
S4	3.357(2)	80.69(7)	93.20(9)	170.93(7)	76.35(6)
	3.318(3)	81.76(9)	93.4(1)	170.6(1)	76.57(9)
Other S	> 3.65				
	3.69				

TABLE 4—*Continued*

	Distance	Angles				
S9	2.425(2)					
	2.412(3)					
S4	2.541(2)	93.51(7)				
	2.535(3)	93.3(1)				
S7	2.676(2)	87.98(7)	94.62(8)			
	2.682(3)	87.8(1)	94.5(1)			
S3	2.914(2)	86.81(7)	93.80(7)	170.35(7)		
	2.890(3)	87.0(1)	93.8(1)	170.4(1)		
S9	3.218(2)	81.87(7)	173.29(7)	90.10(7)	81.13(6)	
	3.224(3)	81.7(1)	173.1(1)	90.1(1)	81.20(9)	
Other S	> 3.73					
	3.76					
Sb6–						
S6	2.434(2)					
	2.424(3)					
S12	2.478(2)	98.40(8)				
	2.482(3)	98.0(1)				
S11	2.610(2)	92.45(8)	94.92(8)			
	2.605(4)	92.6(1)	94.7(1)			
S8	3.070(2)	86.83(7)	80.21(7)	174.91(7)		
	3.040(4)	87.1(1)	80.2(1)	174.8(1)		
S7	3.194(2)	79.14(7)	161.53(7)	103.45(7)	81.37(6)	
	3.164(3)	79.64(9)	162.6(1)	102.7(1)	82.39(9)	
Other S	> 3.59					
	3.62					
Sb7–						
S4	2.464(2)					
	2.460(3)					
S13	2.490(2)	95.95(8)				
	2.486(4)	96.2(1)				
S14	2.502(2)	90.14(9)	90.0(1)			
	2.497(3)	89.8(1)	89.6(2)			
S9	3.139(2)	79.46(7)	87.05(7)	168.81(8)		
	3.131(3)	79.12(9)	87.1(1)	168.0(1)		
S2	3.330(2)	80.89(7)	163.91(7)	105.8(1)	76.87(6)	
	3.358(3)	80.5(1)	164.0(1)	106.0(2)	76.86(8)	
S1	3.442(3)	174.09(7)	81.89(8)	84.37(8)	105.85(6)	102.68(7)
	3.439(4)	174.0(1)	81.9(1)	84.5(1)	106.43(7)	102.9(1)
Other S	> 4.20					
	4.17					
Sb8–						
S11	2.442(2)					
	2.434(4)					
S12	2.466(2)	94.52(8)				
	2.460(3)	94.5(1)				
S5	2.493(2)	93.44(8)	94.31(8)			
	2.480(4)	93.9(1)	94.4(1)			
S12	3.186(2)	82.43(7)	79.38(8)	172.11(7)		
	3.164(4)	82.8(1)	78.8(1)	172.1(1)		
S6	3.348(2)	164.33(7)	77.90(7)	100.73(7)	82.70(6)	
	3.343(3)	164.4(1)	77.68(9)	100.1(1)	82.47(9)	
Other S	> 3.76					
	3.78					

the center of the 4-membered ring (Figs. 2, 3a). Since the 12-membered rings are not flat, the complex chain has a zig-zag shape when viewed laterally.

The crystal structure of **2** is essentially the same as that of **1** (Fig. 3b, Table 4). The Rb atoms are located at positions similar to those of the N atoms in **1**.

The complex pyramidal chains are further interconnected by weak Sb–S bonds (2.88–3.36 Å) into puckered layers that are two atoms thick. The layers are parallel to the (101) plane (Figs. 4, 5a). The shortest Sb–S distance between adjacent layers is 3.44 Å. Wide channel systems along [100] with an aperture of 5.9×8.0 Å are outlined by the 12-membered rings (Fig. 3). The monovalent cations (NH_4^+ and $CH_3NH_3^+$ in **1**, Rb^+ in **2**) and water molecules are located at the intersections of the channels with the interlayer space. The water oxygen atoms OW(2–4) in **1** and OW(4) in **2** are disordered.

The 3-membered rings formed by SbS_3 pyramids are typical building units found in many other thioantimonates. In the structure of $[(CH_3NH_3)_{1.03}K_{2.97}]Sb_{12}S_{20}\cdot 1.34H_2O$, four such 3-membered rings are linked to form a complex loop-branched 8-membered ring (26). In the mineral gerstleyite $Na_2(Sb,As)_8S_{13}\cdot 2H_2O$ (31) and several synthetic compounds such as $(NH_4)_2Sb_4S_7$ (8) and $(enH_2)Sb_8S_{13}$ (18), the 3-membered rings are interconnected into one-dimensional chains that contain 8-membered rings. The 3-membered rings are also found in the structures of $(CH_3NH_3)_2Sb_8S_{13}$ and $(H_3N(CH_2)_3NH_3)Sb_{10}S_{16}$ which are three-dimensional framework structures if the secondary Sb–S bonds are also considered (19, 20).

Close relationships between the structures of **1**, **2**, $[(NH_3CH_2CH_2CH_2NH_2CH_2)_2]_{0.5}Sb_7S_{11}$ (**3**), and $(C_4H_{10}N)_2Sb_8S_{13}\cdot 0.15H_2O$ (**4**) are clearly seen by comparing their two-dimensinal Sb_mS_n layers. Both the 3- and 4-membered rings in the title compounds are found in compound **3** (27). The structure of **4** contains the 4- but not the 3-membered rings (21). As shown in Fig. 5, the three types of layers contain very similar structural blocks although the layer of **1** and **2** is puckered, the layer of **4** flat, and the layer of **3** terraced. The structural blocks are based on an *H*-shaped fragment consisting of 12 SbS_n polyhedra and are indicated by thick solid bonds in Fig. 5. In the

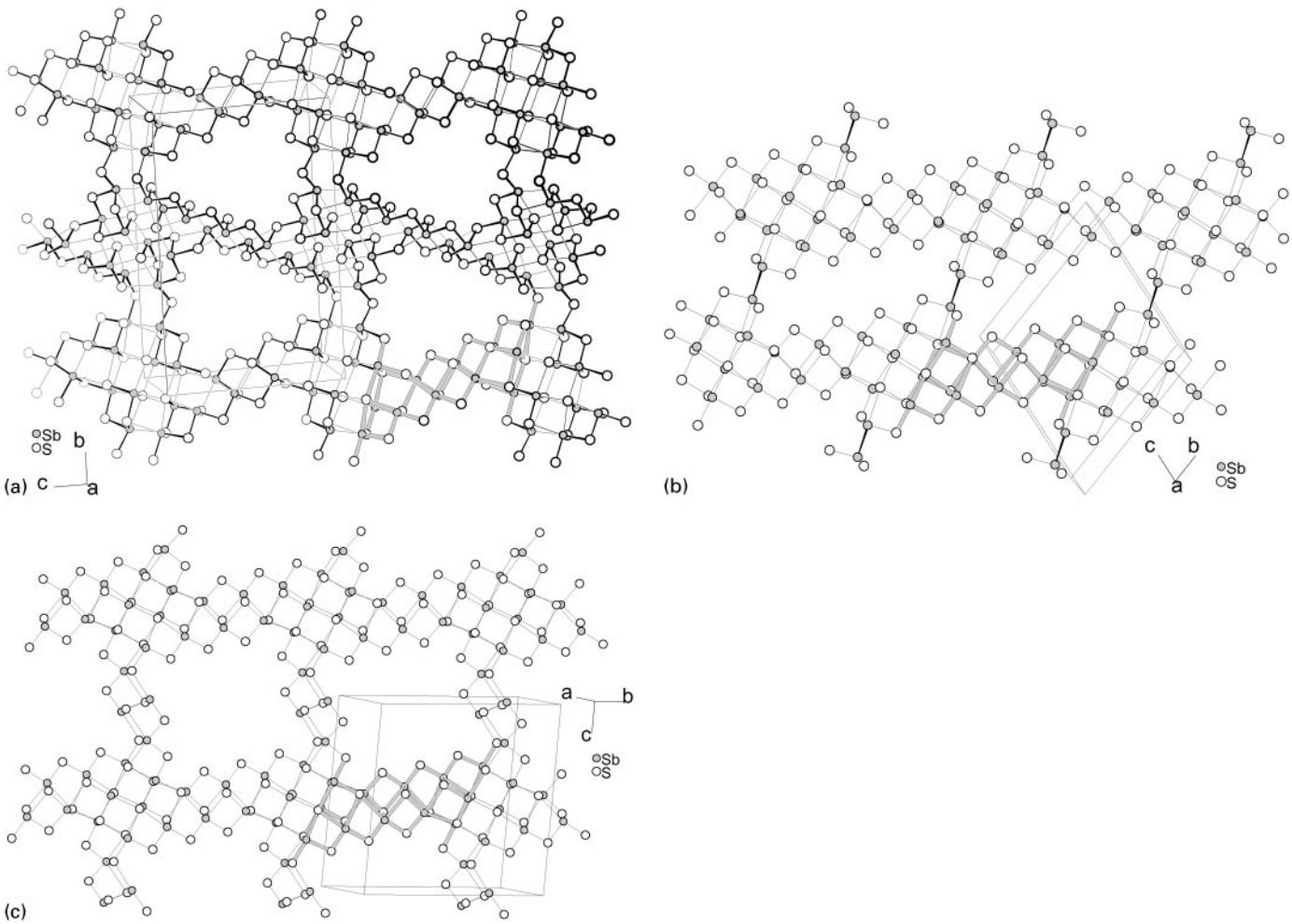

FIG. 5. Antimony sulfide layers in the structures of (a) $[(CH_3NH_3)_{0.5}(NH_4)_{1.5}]Sb_8S_{13}\cdot 2.8H_2O$, (b) $[(NH_3CH_2CH_2CH_2NH_2\ CH_2)_2]_{0.5}Sb_7S_{11}$(27), and (c) $(C_4H_{10}N)_2Sb_8S_{13}\cdot 0.15H_2O$ (21). An *H*-shaped fragment in each structure is indicated by gray solid bonds.

structure of **3**, the *H*-shaped fragments are laterally linked into one-dimensional stripes through Sb–S bonds, and the stripes are linked into the layer by unusual Sb_2 groups with Sb–Sb bonds. The same stripes are cross-linked into layers in **4** by four additional SbS_n polyhedra. In the structure of **1**, the *H*-shaped fragments are interconnected by four additional SbS_n polyhedra into stripes that are similar to but different from those in the layers of **3** and **4**. Adjacent stripes are directly interconnected to form the puckered layer of **1**. The layers of **4** contain square-like 16-membered rings which outline a system of wide channels, with the pyrrolidinium cations and water molecules located at the intersections of the channels, with the interlayer space. In contrast, the layers of **3** contain elongated 12-membered ring pores to accommodate the long-chain cations of protonated *N*,*N*′-bis(3-aminopropyl)ethylenediamine.

In conclusion, two novel thioantimonates have been hydrothermally synthesized. Their crystal structures contain puckered layers and have wide channel systems. Puckered thioantimonate layers are found in many sulfosalt minerals such as $TlSb_5S_8$ (32), but are less common in the synthetic compounds containing alkali metal and organic cations. Since the channels of the structure are filled by water molecules and monovalent cations not larger than methylammonium, measurements of their ion-exchange and adsorption properties are planned.

ACKNOWLEDGMENTS

We thank the National Science Foundation (DMR9805881) and the R. A. Welch Foundation for financial support. This work made use of MRSEC/TCSUH Shared Experimental Facilities supported by the National Science Foundation under Award Number DMR-9632667 and the Texas Center for Superconductivity at the University of Houston.

REFERENCES

1. Lefebvre, M. Lannoo, G. Allan, A. Ibanez, J. Fourcade, J. C. Jumas, and E. Beaurepaire, *Phys. Rev. Lett*. **59,** 2471 (1987).
2. U. Simon, F. Schüth, S. Schunk, X. Wang, and F. Liebau, *Angew. Chem.*, *Int. Ed. Engl.* **36,** 1121 (1997)
3. F. Starrost, E. E. Krasovskii, W. Schattke, J. Jockel, U. Simon, X. Wang, and F. Liebau, *Phys. Rev. Lett*. **80,** 3316 (1998).
4. W. S. Sheldrick and M. Wachhold, *Angew. Chem.*, *Int. Ed. Engl*. **36,** 206 (1997).
5. W. S. Sheldrick and M. Wachhold, *Coord. Chem. Rev*. **176,** 211 (1998).
6. H. A. Graf and H. Schäfer, *Z. Anorg. Allg. Chem.* **414,** 211 (1975).
7. H. A. Graf and H. Schäfer, *Z. Anorg. Allg. Chem.* **414,** 220 (1975).
8. G. Dittmar and H. Schäfer, *Z. Anorg. Allg. Chem.* **437,** 183 (1977).
9. K. Volk and H. Schäfer, *Z. Naturforsch. B* **33,** 827 (1978).
10. G. Dittmar and H. Schäfer, *Z. Anorg. Allg. Chem.* **441,** 98 (1978).
11. K. Volk and H. Schäfer, *Z. Naturforsch. B* **34,** 172 (1979).
12. B. Eisenmann and H. Schäfer, *Z. Naturforsch. B* **34,** 383 (1979).
13. A. S. Kanishcheva, Yu. N. Mikhailov, V. G. Kuznetsov, and V. N. Batog, *Sov. Phys. Dokl.* **25,** 154 (1980).
14. W. S. Sheldrick and H.-J. Häusler, *Z. Anorg. Allg. Chem.* **557,** 105 (1988).
15. W. S. Sheldrick and H.-J. Häusler, *Z. Anorg. Allg. Chem.* **561,** 149 (1988).
16. J. B. Parise, *Science* **251,** 293 (1991).
17. J. B. Parise and Y. Ko, *Chem. Mater*. **4,** 1446 (1992).
18. K. Tan, Y. Ko, and J. B. Parise, *Acta Crystallogr. C* **50,** 1439 (1994).
19. X. Wang and F. Liebau, *J. Solid State Chem.* **111,** 385 (1994).
20. X. Wang, *Eur. J. Solid State Inorg. Chem.* **32,** 303 (1995).
21. Y. Ko, K. Tan, J. B. Parise, and A. Darovsky, *Chem. Mater*. **8,** 493 (1996).
22. K. Tan, Y. Ko, J. B. Parise, J.-H. Park, and A. Darovsky, *Chem. Mater*. **8,** 2510 (1996).
23. W. Bensch and M. Schur, *Eur. J. Solid State Inorg. Chem.* **33,** 1149 (1996).
24. H.-O. Stephan and M. G. Kanatzidis, *J. Am. Chem. Soc*. **118,** 12226 (1996).
25. J. B. Parise, K. Tan, P. Norby, Y. Ko, and C. Cahill, *Mat. Res. Soc. Symp. Proc*. **453,** 103 (1997).
26. X. Wang, A. J. Jacobson, and F. Liebau, *J. Solid State Chem.* **140,** 387 (1999).
27. A. V. Powell, S. Boissiere, and A. M. Chippindale, *Chem. Mater*. **12,** 182 (2000).
28. Siemens Analytical X-ray Instruments: SAINT, Version 4.05, Madison, WI, 1995.
29. G. M. Sheldrick, SADABS program, University of Göttingen, 1995.
30. G. M. Sheldrick, SHELXTL, Version 5.03, Siemens Analytical X-ray Instruments, Madison, WI, 1995.
31. I. Nakai and D. Appleman, *Chem. Lett*. **1981,** 1327 (1981).
32. P. Engel, *Z. Kristallogr*. **151,** 203 (1980).